Title

Designing New Magnesium Pincer Complexes for Catalytic Hydrogenation of Imines and N-Heteroarenes: H2 and N-H Activation by Metal-Ligand Cooperation as Key Steps.

Journal

Journal of the American Chemical Society, 145(16)

Authors

Liang, Yaoyu

Luo, Jie

Diskin-Posner, Yael

et al.

Publication Date

2023-04-26

DOI

10.1021/jacs.3c01091

Peer reviewed

JACS
JOURNAL OF THE AMERICAN CHEMICAL SOCIETY
pubs.acs.org/JACS
Article

Designing New Magnesium Pincer Complexes for Catalytic Hydrogenation of Imines and *N*-Heteroarenes: H_2 and N−H Activation by Metal−Ligand Cooperation as Key Steps

Yaoyu Liang, Jie Luo, Yael Diskin-Posner, and David Milstein*

Cite This: *J. Am. Chem. Soc.* 2023, 145, 9164−9175
Read Online
ACCESS | Metrics & More | Article Recommendations | Supporting Information

ABSTRACT: Utilization of main-group metals as alternatives to transition metals in homogeneous catalysis has become a hot research area in recent years. However, their application in catalytic hydrogenation is less common due to the difficulty in heterolytic cleavage of the H−H bond. Employing aromatization/de-aromatization metal−ligand cooperation (MLC) highly enhances the H_2 activation process, offering an efficient approach for the hydrogenation of unsaturated molecules catalyzed by main-group metals. Herein, we report a series of new magnesium pincer complexes prepared using PNNH-type pincer ligands. The complexes were characterized by NMR and X-ray single-crystal diffraction. Reversible activation of H_2 and N−H bonds by MLC employing these pincer complexes was developed. Using the new magnesium complexes, homogeneously catalyzed hydrogenation of aldimines and ketimines was achieved, affording secondary amines in excellent yields. Control experiments and DFT studies reveal that a pathway involving MLC is favorable for the hydrogenation reactions. Moreover, the efficient catalysis was extended to the selective hydrogenation of quinolines and other *N*-heteroarenes, presenting the first example of hydrogenation of *N*-heteroarenes homogeneously catalyzed by early main-group metal complexes. This study provides a new strategy for hydrogenation of C═N bonds catalyzed by magnesium compounds and enriches the research of main-group metal catalysis.

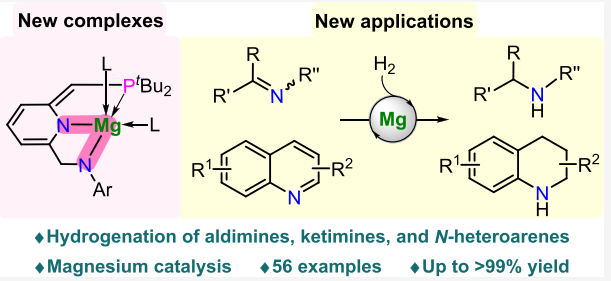

INTRODUCTION

Catalytic hydrogenation of unsaturated molecules by H_2 is one of the most practical transformations in laboratory and industry.[1] Classic catalysts mainly rely on late transition metals due to their efficiency in the cleavage of H_2.[1,2] Due to the toxic and costly characteristics, it is increasingly interesting to use cheaper and more environmentally benign catalysts, such as the first-row transition metal compounds and frustrated Lewis pairs (FLPs).[3−5] However, as another large group of elements in the periodic table, the main-group metals have received much less attention in catalytic hydrogenation due to their lack of partially filled d orbitals and the instability of many main-group metal compounds, which largely impeded their application in bond activation.[6−12] In the 1960s, simple metal hydrides and inorganic bases were known as catalysts for the hydrogenation of benzophenone, alkenes, and alkynes, but harsh conditions were required.[7] In 2008, Harder and co-workers reported a β-diketiminate calcium hydride complex and K, Ca, and Sr benzyl catalysts, providing relatively mild conditions for the catalytic hydrogenation of conjugated alkenes (Figure 1a).[8a] Subsequently, Okuda's group developed the hydrogenation of non-activated alkenes catalyzed by cationic calcium hydride complexes.[8b,c] Cheng et al. reported the bulky penta-arylcyclopentadienyl ligand-supported heavy alkaline earth metals (Ca, Sr, and Ba) hydrides that exhibited activity in the hydrogenation of various alkenes.[8e−g] Recently, group 1 and group 2 metal amides have been prepared for the catalytic hydrogenation of challenging alkenes and extended to imine hydrogenation.[9] In addition, cationic β-diketiminate aluminum complexes were found to be efficient catalysts in the hydrogenation of imines.[10] Several heterobimetallic systems also exhibited capability in activation of H_2 and efficiency in hydrogenation of alkenes and imines.[11] Very recently, magnesium pincer complex-catalyzed semihydrogenation of alkynes and hydrogenation of alkenes were reported by our group.[12] Despite continuous breakthroughs in the main-group metal-catalyzed hydrogenation, it is not on par with the classical transition metal catalysts. Thus, enriching the main-group metal catalysis (especially by the abundant early main-group metals) to broaden their application in hydrogenation is still highly necessary.

Received: January 30, 2023
Published: April 17, 2023

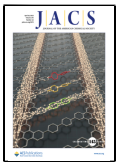

https://doi.org/10.1021/jacs.3c01091
J. Am. Chem. Soc. 2023, 145, 9164−9175

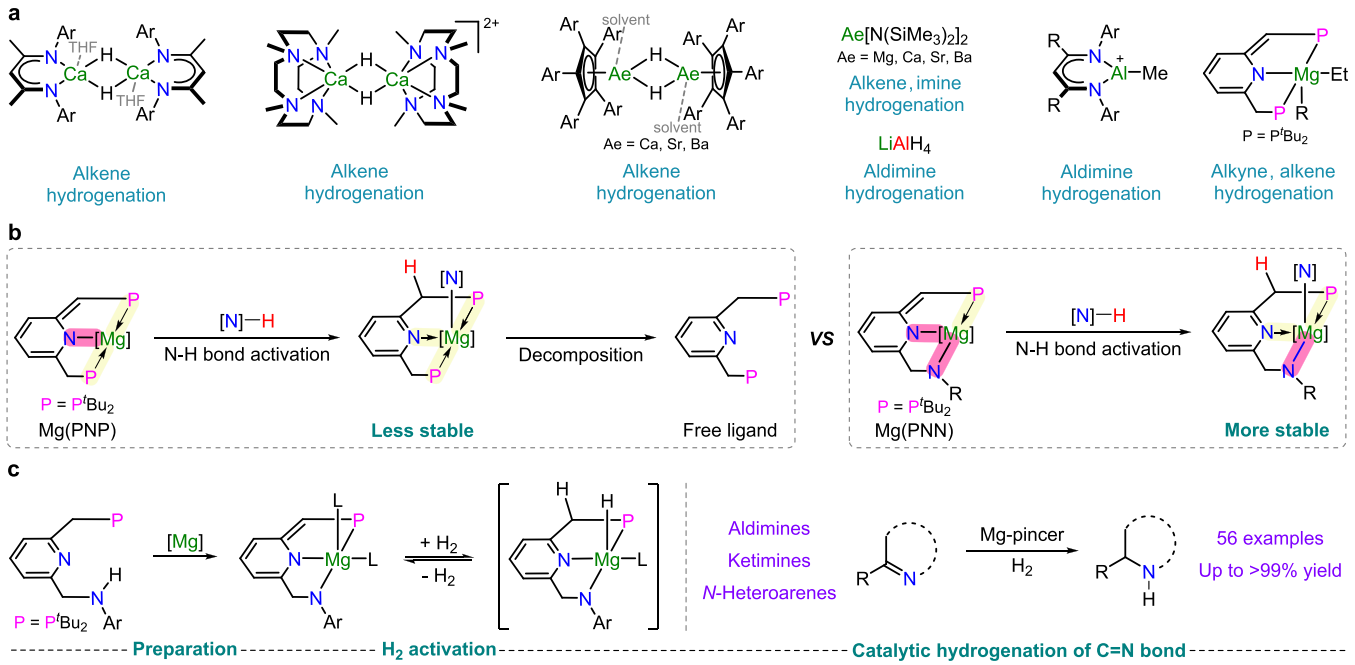

Figure 1. Overview of this work. (a) Representative main-group metal complexes for hydrogenation of unsaturated molecules. (b) Comparison of the Mg(PNP) complex with the new Mg(PNN) complex. (c) This work, preparation of new magnesium pincer complexes, and their application in reversible activation of H_2 and catalytic hydrogenation of the C═N bond.

In the specific area of hydrogenation, the reduction of imines by H_2 offers an atom-economic approach to access amines (linear and cyclic).[13] Although various catalysts based on FLPs[5d] and sustainable metals[4,9b,c,10,11a,c,d,14,15] have been developed to avoid using expensive and toxic metals, examples of using early main-group metals are scarce.[9b,c,11d] In 2018, Harder's group reported the first successful example of hydrogenation of imines catalyzed by alkaline earth and alkali metal amides via a metal hydride mechanism.[9b] While this system is active with aldimines and inefficient with ketimine substrates, further studies by the same group and by Pfaltz et al. reported that substoichiometric amounts of LiHMDS and 100 bar of H_2 were required to ensure high yield.[9c] Magnesium, in these cases, exhibited lower catalytic activity than heavy alkaline earth metals.

In recent years, magnesium compounds have emerged as redox-neutral catalysts for a variety of reactions[6,16−20] such as hydroamination,[17] hydrosilylation,[18] hydroboration,[19] and dehydrocoupling.[20] However, the application in hydrogenation is still challenging because of its lower efficiency in activating the H−H bond.[9b,11d,12] Metal−ligand cooperation (MLC) involving aromatization/de-aromatization of pincer metal complexes offers a versatile tactic for activating small molecules.[2d,21] Recently, we developed a series of de-aromatized (with a deprotonated side arm) magnesium pincer complexes supported by PNP-, PNN-, and NNN-type ligands.[12] We showed that a Mg(PNP) complex is capable of reversible heterolysis of H_2 via an MLC process and catalyzes the hydrogenation of unsaturated C−C bonds, providing a new strategy for enhancing the catalytic activity of magnesium compounds. Nevertheless, the de-aromatized complex is incompatible with compounds that contain active protons, such as amines, since the derived aromatized (with fully protonated side arms) intermediate from the N−H bond activation is unstable due to the weakly coordinating phosphines of the (PNP)^{t}Bu ligand and the magnesium center (Figure 1b, left). To meet the requirement of C═N bond hydrogenation, we speculated that using PNNH-type ligands can construct a more stable Mg(PNN) complex that may be compatible with amine products since the aromatized intermediate from the N−H bond activation would bear a stronger covalent Mg−N bond, which can stabilize the intermediate (Figure 1b, right).

Herein, we report the preparation of a series of new magnesium pincer complexes using PNNH-type ligands (Figure 1c, left). The amine proton of the PNNH ligand was replaced by magnesium, forming a new Mg−N covalent bond, further stabilizing the complexes. The activation of H−H and N−H bonds via the MLC process was studied. Catalytic hydrogenation of various aldimines and ketimines was proved feasible, generating secondary amines in up to >99% yields (Figure 1c, right). A plausible mechanism involving an MLC process is proposed on the basis of control experiments and DFT studies. The developed catalytic system is also efficient in the selective hydrogenation of a variety of *N*-heteroarenes, generating cyclic amines in high yields.

RESULTS AND DISCUSSION

Preparation and Characterization of Magnesium Pincer Complexes. The aromatized magnesium bromide complex **Mg-1a** was prepared by the reaction of the PNNH-type ligand (**L1**) with EtMgBr in Et_2O (Figure 2a, left). A yellowish precipitate was formed after stirring the solution at room temperature for 5 h. The solid is soluble in THF, generating complex **Mg-1a** with a coordinated THF molecule. The $^{31}P\{^1H\}$ NMR spectrum of **Mg-1a** exhibits a singlet at 22.89 ppm, suggesting formation of an aromatized structure, in line with the reported chemical shifts in previous studies.[12,22] Two methylene (CH_2) groups of the phosphine and amine side arms were observed by ^1H NMR, supporting the aromatized structure. Single crystals of **Mg-1a** suitable for X-ray diffraction studies were grown at room temperature. X-ray

https://doi.org/10.1021/jacs.3c01091
J. Am. Chem. Soc. 2023, 145, 9164−9175

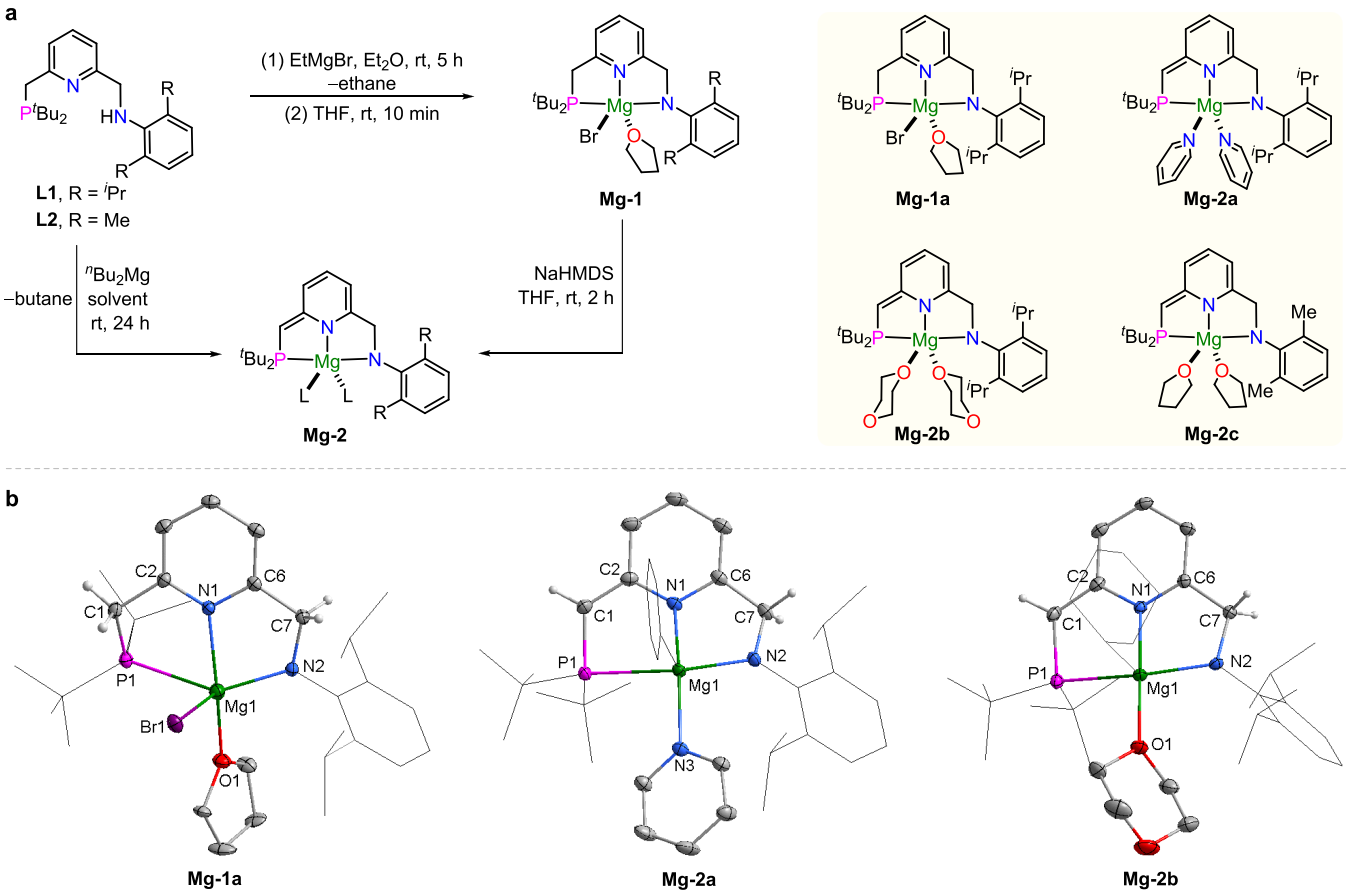

Figure 2. Preparation and characterization of magnesium pincer complexes. (a) Procedures for preparing magnesium pincer complexes and the obtained complexes. (b) Crystal structures of complexes **Mg-1a** (left), **Mg-2a** (middle), and **Mg-2b** (right). Selected hydrogen atoms were omitted for clarity. Some groups were displayed as wireframes for clarity. Selected bond lengths (Å) and angles (deg): (**Mg-1a**) Mg1−P1 2.8367(6), Mg1−N1 2.1594(12), Mg1−N2 1.9939(13), Mg1−O1 2.0554(12), Br−Mg1 2.5120(5), C1−C2 1.503(2), C6−C7 1.499(2), Br1−Mg1−O1 99.83(4), Br1−Mg1−N2 122.21(4), and Br1−Mg1−P1 99.047(17). (**Mg-2a**) Mg1−P1 2.7644(5), Mg1−N1 2.1086(10), Mg1−N2 2.0129(10), C1−C2 1.3857(16), C6−C7 1.5052(16), and N3−Mg1−N4 94.25(4). (**Mg-2b**) Mg1−P1 2.7335(4), Mg1−N1 2.0700(9), Mg1−N2 2.0151(9), C1−C2 1.3967(15), C6−C7 1.5155(14), and O1−Mg1−O3 90.91(3).

crystallography reveals that **Mg-1a** is formed as a five-coordinated complex, in line with many reported examples (Figure 2b, left).[12,18c,23] The bromo group and the THF ligand formed at a 99.8° angle (Br1−Mg1−O1). The bond length of Mg1−N2 (1.99 Å) is considerably shorter than that of Mg1−N1 (2.16 Å), suggesting the formation of a Mg−N covalent bond between Mg1 and N2, which differed from the reported transition-metal complexes prepared by PNNH-type ligands that possessed a free amine proton.[24] It is noted that an analogous aromatized structure was not observed in previous PNP magnesium complexes, confirming that the covalent bond between Mg1 and N2 is crucial for stabilizing the aromatized structure.

Next, an equivalent amount of base (NaHMDS) was added to the THF solution of **Mg-1a** in order to deprotonate the side arm and remove the bromo group. A white precipitate gradually formed during the reaction, implying the generation of sodium bromide. A singlet was observed at 3.15 ppm in the $^{31}P\{^{1}H\}$ NMR spectrum after the full consumption of **Mg-1a**, revealing that the deprotonation only took place at the phosphine side arm to generate a single product. Removing the solvent provided thick oil, which is soluble in pyridine or dioxane to yield the de-aromatized complexes **Mg-2a** and **Mg-2b** with pyridine and dioxane, respectively, as additional ligands (Figure 2a, right). The $^{31}P\{^{1}H\}$ NMR spectra of **Mg-2a** and **Mg-2b** exhibit similar singlets at 2.66 and 3.35 ppm, respectively. The chemical shifts suggest that they are de-aromatized structures. The methine (*CH*) signals of the phosphine side arms of **Mg-2a** and **Mg-2b** were observed at 3.69 (d, J = 5.1 Hz) and 3.16 (d, J = 4.9 Hz) ppm by ^{1}H NMR. X-ray crystallography of **Mg-2a** shows a considerably shorter C1−C2 bond (1.39 Å) compared to the C6−C7 bond (1.51 Å), supporting its de-aromatized structure. Two pyridine ligands are coordinated to the magnesium center at a 94.3° angle, similar to that of aromatized **Mg-1a**. Likewise, a shorter C1−C2 bond (1.40 Å) compared to a C6−C7 bond (1.52 Å) can be observed in the X-ray structure of **Mg-2b**. Following similar two-step procedures using **L2** as a ligand, a de-aromatized complex **Mg-2c** was obtained with two THF ligands coordinated to the magnesium center. The $^{31}P\{^{1}H\}$ NMR spectrum exhibits a singlet at 4.04 ppm, similar to that of **Mg-2a** and **Mg-2b**. The ^{1}H NMR spectrum exhibits a characteristic doublet at 3.55 ppm (J = 5.2 Hz, 1H) and a singlet at 4.43 ppm (2H), which are assigned to the methine (*CH*) and methylene (CH_2) of the phosphine side arm and amine side arm, respectively, confirming the de-aromatized structure. Signals assigned to two THF ligands were also observed by ^{1}H NMR, supporting the structure of **Mg-2c**. It

https://doi.org/10.1021/jacs.3c01091
J. Am. Chem. Soc. 2023, 145, 9164−9175

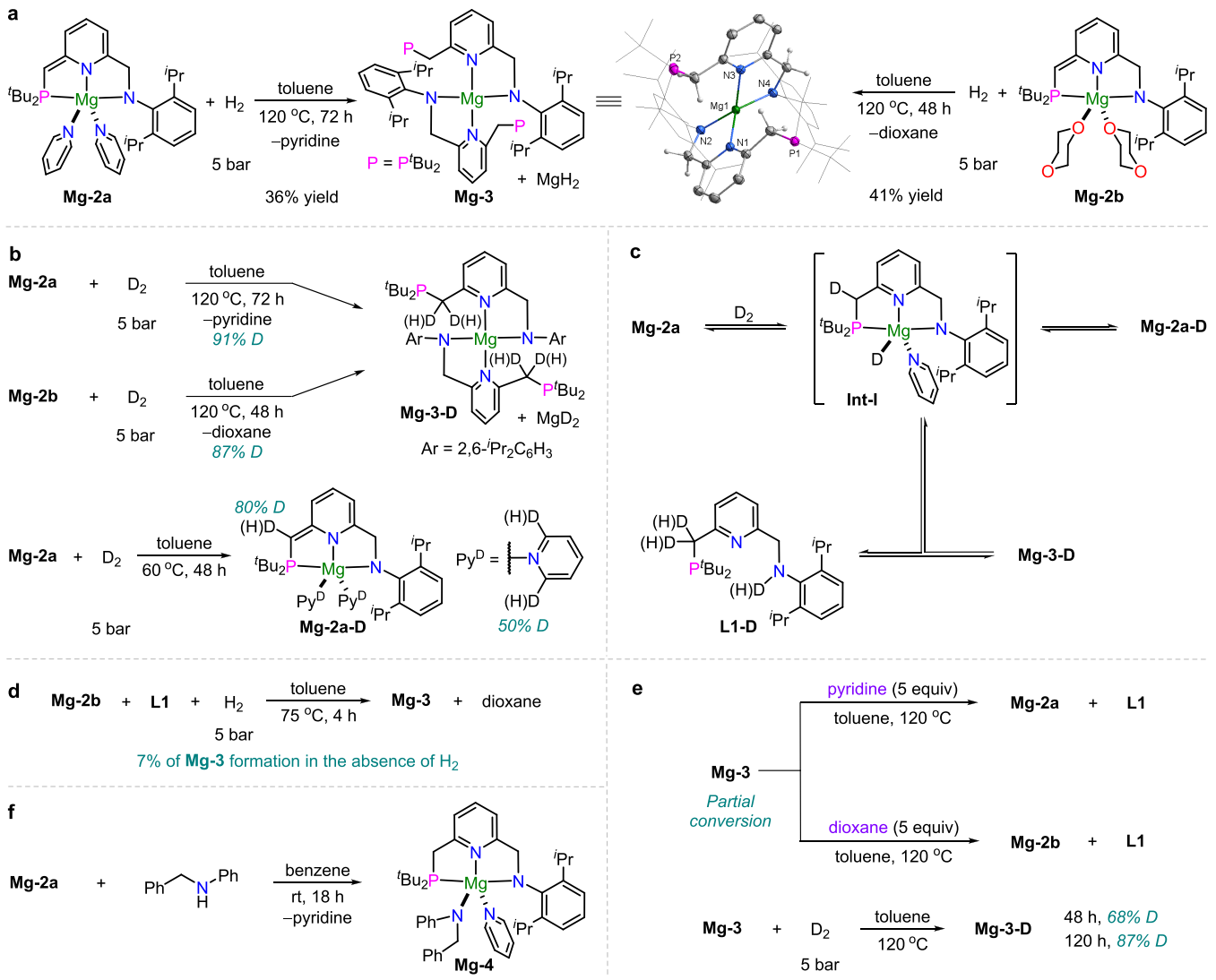

Figure 3. Studies of H_2 (D_2) and amine activation by de-aromatized complexes. (a) Formation of **Mg-3** by the reaction of **Mg-2a** and **Mg-2b** with H_2. (b) Formation of **Mg-3-D** by the reaction of **Mg-2a** and **Mg-2b** with D_2. (c) Proposed pathway for the reversible activation of D_2 by **Mg-2a**. (d) Control experiments to confirm that H_2 is required for the generation of **Mg-3**. (e) Conversion of **Mg-3** to de-aromatized complexes and the free ligand and activation of D_2 by **Mg-3**. (f) Activation of the N–H bond by **Mg-2a**.

should be mentioned that **Mg-2c** is less stable than **Mg-2a** and **Mg-2b**, possibly due to the lower steric hindrance of the anilido ligand. In addition, a one-step procedure to access the de-aromatized complexes from ligands **L1** and **L2** was developed by using ^{n}Bu$_2$Mg as a precursor. The deprotonation occurs by the generated butyl ligand, avoiding the use of an additional base and generating 2 equiv of butane as the only byproduct. Following this procedure, **Mg-2b** and **Mg-2c** were obtained at room temperature using dioxane or THF as solvents. However, a trace amount of de-aromatized product originating from deprotonation of the amine side arm was observed by NMR as well.

Bond Activation by Magnesium Pincer Complexes. To test the ability of the de-aromatized complexes for H_2 activation, a toluene solution of **Mg-2a** was treated with 5 bar of H_2 in a J. Young NMR tube (Figure 3a, left). Heating at 120 °C, the orange solution turned green. A new species with a $^{31}P\{^1H\}$ NMR signal at 20.81 ppm was gradually formed, suggesting that an aromatized compound may be formed. After the full consumption of **Mg-2a**, the ^1H NMR showed two characteristic methylene (CH_2) signals assigned to the phosphine and amine side arms, verifying the formation of an aromatized structure. Single crystals of the new species were obtained at room temperature using a mixed solvent of THF/pentane. X-ray crystallography confirmed the structure as **Mg-3**, a four-coordinated dimer with two PNN ligands and uncoordinated phosphorous atoms. Similarly, **Mg-2b** fully converted into the dimer complex **Mg-3** under H_2 pressure with shorter reaction time, implying its higher activity (Figure 3a, right). These results suggested that the de-aromatized complexes **Mg-2a** and **Mg-2b** may undergo activation of H_2 by MLC, as reported in the case of a Mg(PNP) complex.[12] To confirm that, a toluene solution of **Mg-2a** was pressurized with 5 bar of D_2 and heated at 120 °C in a J. Young NMR tube (Figure 3b, top). After the full consumption of **Mg-2a**, **Mg-3-D** was obtained with deuterium signals on the phosphine side arm of **Mg-3**, as confirmed by ^2H NMR (Figure S38). It was found that 91% of deuterium was incorporated into the phosphine side arm according to the integration of the ^1H NMR (Figure S39). Likewise, the treatment of **Mg-2b** with D_2

https://doi.org/10.1021/jacs.3c01091
J. Am. Chem. Soc. 2023, 145, 9164–9175

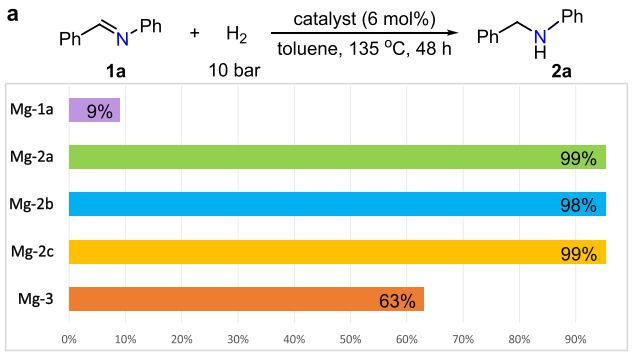

b

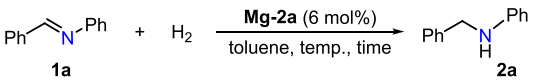

entry	H_2 (bar)	temp. (°C)	time (h)	yield (%)
1	10	135	48	99
2	7	135	48	97
3	5	135	48	91
4	10	150	48	>99
5	10	120	48	85
6	10	135	60	>99
7	10	135	36	95
8	10	135	24	88

c

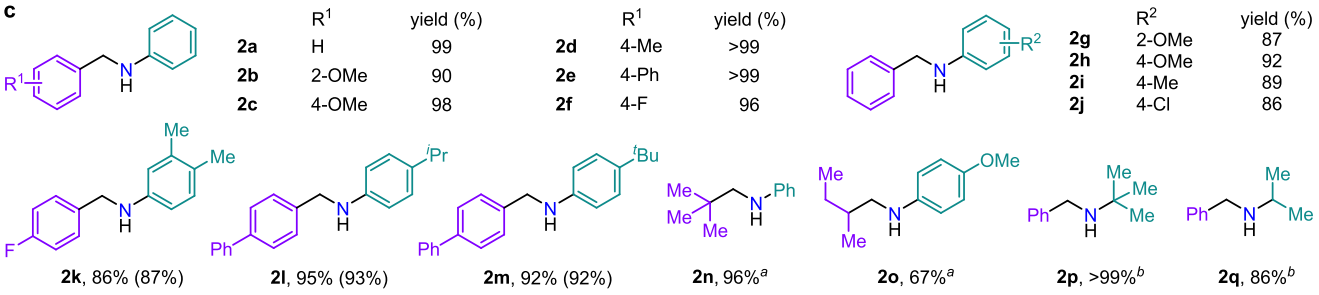

Figure 4. Catalytic hydrogenation of aldimines. (a) Effect of different magnesium complexes. (b) Effect of hydrogen pressure, reaction temperature, and reaction time. (c) Scope of aldimines. Reaction conditions: **1** (0.3 mmol), **Mg-2a** (6 mol %), H_2 (10 bar), toluene (1 mL), 135 °C, 48 h. Reaction yields were determined by ^{1}H NMR spectroscopy of the crude reaction mixture with respect to 1,3,5-trimethoxybenzene as an internal standard. Isolated yields are in parentheses. Superscript a signifies that 10 mol % of **Mg-2b** was used as the catalyst at 150 °C. Superscript b signifies that 6 mol % of **Mg-2b** was used as the catalyst.

under similar conditions produced **Mg-3-D** with 87% of the deuterated phosphine side arm (Figure S42). These results show that the de-aromatized complexes **Mg-2a** and **Mg-2b** can reversibly activate D_2 (H_2). In addition, upon treatment of a toluene solution of **Mg-2a** with 5 bar of D_2 at a lower temperature (60 °C), **Mg-2a-D** was formed with 80% deuterium incorporated into the phosphine side arm of **Mg-2a** after 48 h, further confirming the reversible activation of D_2 (H_2) by the de-aromatized complexes (Figure 3b, bottom). It is noteworthy that in the above results, the deuteration of the amine side arm was not observed, in line with the observation in the preparation process that the protons on the phosphine side arm undergo deprotonation more readily.

The generation of **Mg-3-D** and **Mg-2a-D** likely proceeds via the aromatized intermediate **Int-I**, which is derived from the reaction of **Mg-2a** with D_2 (Figure 3c). **Int-I** was not observed during the reaction since it quickly underwent the elimination of DH (or D_2) to generate **Mg-2a-D** (or **Mg-2a**) to enter the next cycle of D_2 activation. Meanwhile, the instability of **Int-I** resulted in partial decomposition in the presence of D_2 to produce the deuterium-labeled free ligand **L1-D**, which reacted with **Int-I** to generate the dimer complex **Mg-3-D**. Theoretically, the reaction of the ligand **L1-D** with **Mg-2a** (or **Mg-2a-D**) can produce the dimer complex **Mg-3-D** via the deuterium (proton) transfer from amine to the de-aromatized phosphine side arm without the participation of D_2 (H_2). To clarify this point, a toluene solution of **Mg-2b** and **L1** was heated in the presence of H_2 (5 bar) at 75 °C, resulting in the formation of **Mg-3** after 4 h (Figure 3d). On the contrary, only about 7% of **Mg-3** can be observed in the absence of H_2 under the same conditions. These results suggest that H_2 is required for the formation of **Mg-3** and indirectly confirm the formation of the active intermediate **Int-I**.

The dimer complex **Mg-3** is unstable in the absence of H_2. Upon treatment of **Mg-3** with 5 equiv of pyridine or dioxane at 120 °C, the dearomatized complexes **Mg-2a** and **Mg-2b** were gradually regenerated together with the formation of free ligand **L1** (Figure 3e, top). The decomposition of **Mg-3** originated from the deprotonation of the phosphine side arm by the anilido ligand of the complex itself. As a result, the free ligand can be observed along with the formation of de-aromatized complexes. However, the consumption of **Mg-3** is incomplete (Figures S45 and S46), even upon prolonging the reaction time to 2 days, suggesting the existence of an equilibrium between the dimer, the de-aromatized complexes, and the free ligand. To confirm that, a toluene solution of **Mg-3** was treated with D_2 and heated at 120 °C (Figure 3e, bottom), resulting in the incorporation of 68% of deuterium into the phosphine side arm after 48 h (Figure S47), and the deuterated ratio increased to 87% after 5 days (Figure S49). This result confirms that the formation of **Mg-3** is reversible.

The activation of the N−H bond by the de-aromatized complexes was studied as well. Upon treatment of the benzene solution of **Mg-2a** with *N*-benzylaniline in a J. Young NMR tube, a singlet can be observed at 24.87 ppm in the ^{31}P{^{1}H} NMR spectrum after rotating the tube for 18 h at room temperature. The chemical shift of the signal implies the generation of an aromatized species (Figure 3f). In the ^{1}H NMR, a doublet (J = 2.9 Hz) assigned to the methylene (CH_2) group of the phosphine side arm was found at 2.99 ppm, confirming the aromatized structure of the generated magnesium complex. The methylene (CH_2) signals of the amine side arm and the benzyl group of *N*-benzylaniline were also found at 5.06 and 4.75 ppm, respectively. The ^{1}H NMR exhibits one pyridine ligand, suggesting that the secondary amine replaced a pyridine ligand to generate a new Mg−N covalent bond. The new complex was finally confirmed as **Mg-**

https://doi.org/10.1021/jacs.3c01091
J. Am. Chem. Soc. 2023, 145, 9164−9175

Table 1. Scope of Magnesium-Catalyzed Hydrogenation of Ketimines[a]

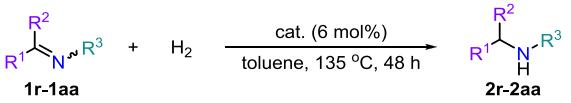

1r-1aa 2r-2aa

entry	ketimine	cat.	amine	yield (%)[b]
1	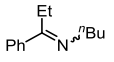 1r	Mg-2a	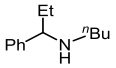 2r	96
2	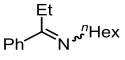 1s	Mg-2b	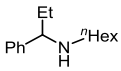 2s	>99
3[c]	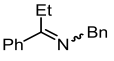 1t	Mg-2b	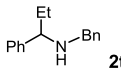 2t	97
4	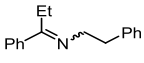 1u	Mg-2a	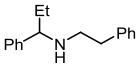 2u	99[d]
5[c,e]	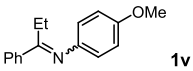 1v	Mg-2b	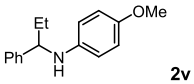 2v	85[d]
6	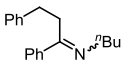 1w	Mg-2b	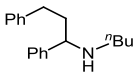 2w	98
7	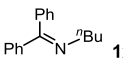 1x	Mg-2b	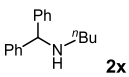 2x	>99
8	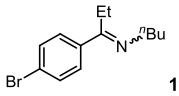 1y	Mg-2b	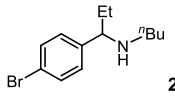 2y	92[d]
9	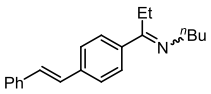 1z	Mg-2b	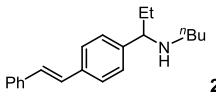 2z	98[d]
10	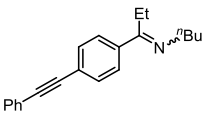 1aa	Mg-2b	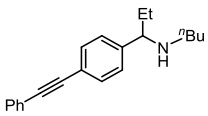 2aa	95[d]

[a]Conditions: **1** (0.3 mmol), cat. (6 mol %), H_2 (10 bar), toluene (1 mL), 135 °C, 48 h. [b]Yield determined by ^{1}H NMR spectroscopy of the crude reaction mixture with respect to 1,3,5-trimethoxybenzene as an internal standard. [c]The reaction temperature was 150 °C. [d]Isolated yield. [e]With 10 mol % of catalyst.

4, which was derived from the N−H bond activation by **Mg-2a** via the MLC process.[25] It should be mentioned that the analogous structure could not be observed by using previously reported PNP magnesium complexes (see page S53 in the SI),[12] indicating that the current complexes are more stable.

Catalytic Hydrogenation of Imines. As the reversible activation of H_2 (D_2) by **Mg-2a** and **Mg-2b** via the MLC process was shown to be feasible and activation of a secondary amine by **Mg-2a** was observed as well, we believed that hydrogenation of imines catalyzed by the new magnesium complexes might be possible. Examining this possibility, commercially available (*E*)-*N*,1-diphenylmethanimine (**1a**) was employed as a substrate to test the catalytic activity of the obtained magnesium complexes (Figure 4a). High conversion of **1a** was observed using 6 mol % of the de-aromatized **Mg-2a** as a catalyst, generating the desired amine **2a** in 99% yield after heating at 135 °C for 48 h under 10 bar of H_2. The de-aromatized complexes **Mg-2b** and **Mg-2c** exhibited similar catalytic activity in the hydrogenation of **1a**, resulting in 98 and 99% yield of **2a**, respectively. However, the aromatic magnesium bromide complex **Mg-1a** (which is incapable of de-aromatization in the absence of base) showed much lower activity (9% yield), indicating the importance of the de-aromatized structure in H_2 activation. As expected, the dimeric complex, **Mg-3**, can catalyze the imine hydrogenation, resulting in the desired amine **2a** in 63% yield under standard conditions. The result is in line with the observation that **Mg-3** can slowly be converted into the de-aromatized complexes, which act as the active catalysts for hydrogenation. However, the lower conversion of **1a** suggests that the formation of **Mg-3** deactivates the de-aromatized catalysts. These results also indicate that the de-aromatized complexes **Mg-2a**, **Mg-2b**, and **Mg-2c** were only partially converted into the dimer in the catalytic process. Other reaction parameters for the hydrogenation of **1a** were also explored by using **Mg-2a** as a catalyst (Figure 4b). Lower hydrogen pressures (7 and 5 bar) only slightly affected the reaction yields (97 and 91%). However, the temperature and reaction time significantly influence the reaction. Increasing the temperature to 150 °C led to full consumption of **1a**, affording **2a** in >99% yield after 48 h. Decreasing the temperature to 120 °C provided 85% yield of **2a** after 48 h. Upon prolonging the reaction time to 60 h, the imine **1a** was completely converted into the secondary amine. Reducing the reaction time to 36 and 24 h resulted in 95 and 88% yields, respectively. These results are encouraging since

https://doi.org/10.1021/jacs.3c01091
J. Am. Chem. Soc. 2023, 145, 9164−9175

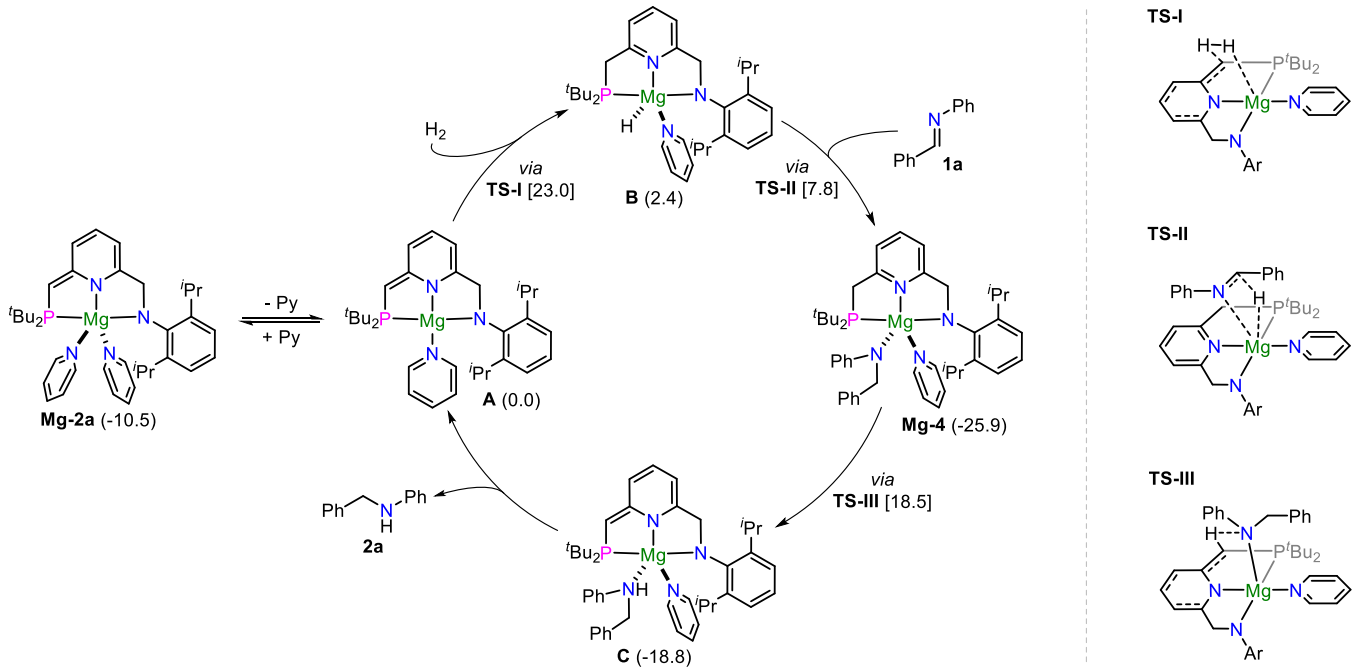

Figure 5. Proposed mechanism for hydrogenation of imines catalyzed by de-aromatized magnesium complexes. In parentheses, the relative free energies (in kcal/mol) of intermediates with respect to active intermediate **A** as 0.0 kcal/mol are given. In square brackets, the activation free energy barriers for the corresponding steps are given.

magnesium-catalyzed hydrogenation of *N*-aryl aldimines in high yields is still challenging.[9b,]

With the optimal conditions in hand, the scope of aldimines was explored (Figure 4c). Using **Mg-2a** as a catalyst, a variety of *N*-aryl arylaldimines bearing different substituents smoothly afforded the desired amines (**2a**-**2m**) in high yields (86 to >99%). Aromatic aldimines having substituents at the *para*-position gave higher yields than the *ortho*-OMe-substituted one (**2c**−**2f** vs **2b**). Placing the OMe group at the *ortho*-position of the *N*-aryl group also resulted in a lower yield (**2g**, 87%). Placing different substituents on both aryl rings of *N*-aryl arylaldimines did not affect the reaction, affording the desired products in 86−95% yields (**2k**-**2m**). The reaction tolerated various functional groups, such as methoxy, fluoro, and chloro, which are generally sensitive toward common magnesium compounds. Likewise, aliphatic *N*-aryl aldimines were suitable for hydrogenation, but a higher catalyst loading (10 mol %) and higher reaction temperature (150 °C) were required due to the less electrophilic C═N bond. Using **Mg-2b** as a catalyst, tertiary butyl-substituted imine **1n** successfully afforded the corresponding amine **2n** in 96% yield. Interestingly, *sec*-butyl-substituted aldimine gave only 67% yield of **2o**. Prolonging the reaction time did not efficiently improve the conversion. This result indicates that significant steric hindrance was required to ensure high yields of the aliphatic aldimines. Additionally, *N*-alkyl aldimines also gave rise to the corresponding amines in high yields. For example, the (*E*)-*N*-*tert*-butyl-1-phenylmethanimine (**1p**) with large steric hindrance efficiently generated **2p** in >99% yield catalyzed by **Mg-2b**. Replacing the tertiary butyl group with the smaller isopropyl group resulted in a lower yield (**2q**, 86%). The results of hydrogenating aliphatic aldimines and *N*-alkyl aldimines suggest that the steric hindrance of the generated amines is related to the reaction yields due to the de-aromatized complexes being more compatible with bulky amines. The above results indicate that the developed magnesium pincer complexes are efficient in the hydrogenation of various aldimines, generating much better results than previously reported magnesium catalysis.[9b,11d]

Next, the catalytic hydrogenation of ketimines by the de-aromatized magnesium complexes was explored (Table 1). It is noted that the hydrogenation of ketimines catalyzed by early main-group metal complexes is challenging due to the larger steric hindrance compared to aldimines.[9b] Employing **Mg-2a** as a catalyst, the simple ketimine **1r** was successfully converted into the secondary amine **2r** in 96% yield. Ketimines (**1s**−**1u**) bearing different chain lengths of *N*-alkyl substituents also gave quantitative yields (97 to >99%). Steric hindrance appears to be an important factor in the reaction. For example, the *N*-aryl-substituted ketimine **1v** generated amine **2v** in a lower yield (85%), catalyzed by 10 mol % of **Mg-2b** at 150 °C. Replacing the substituents on the carbon atom of the ketimines by phenethyl and phenyl groups, the reactions were successfully performed to produce **2w** and **2x** in 98 and >99% yield, respectively. Interestingly, the bromo group and C−C double and triple bonds were not affected by the current conditions, generating the desired products **2y**−**2aa** in 92−98% isolated yields. It is worth mentioning that both *E*- and *Z*-ketimines efficiently undergo hydrogenation in this system, providing a new strategy for the hydrogenation of mixed imines of *Z* and *E* configurations.

Proposed Mechanism. A plausible pathway for the hydrogenation of imines is proposed on the basis of the above experiments and supported by DFT studies (Figure 5). The reaction starts with the reversible dissociation of one pyridine ligand from **Mg-2a** to generate the four-coordinated intermediate **A**, which provides a vacant site for the activation of hydrogen. This step is an endergonic process with ΔG = 10.5 kcal/mol according to the DFT calculations. H_2 activation by de-aromatized intermediate **A** generates the five-coordinated aromatized magnesium hydride intermediate **B**. The activation proceeds via transition state **TS-I**, in which the H_2

https://doi.org/10.1021/jacs.3c01091
J. Am. Chem. Soc. 2023, 145, 9164−9175

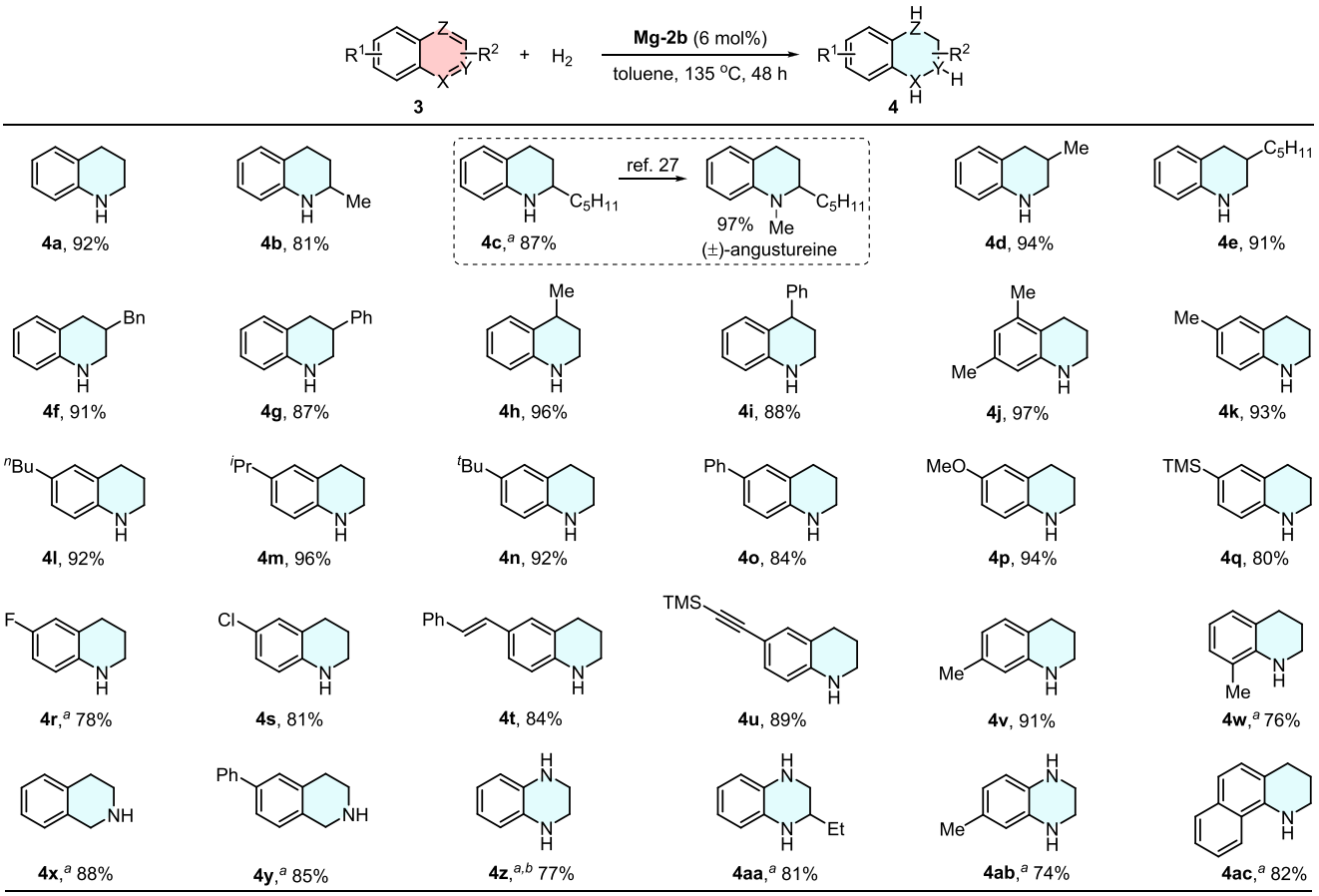

Figure 6. Catalytic hydrogenation of *N*-heteroarenes. Reaction conditions: **3** (0.3 mmol), **Mg-2b** (6 mol %), H_2 (10 bar), toluene (1 mL), 135 °C, 48 h. The yields refer to isolated yields. Superscript a signifies that the reaction temperature was 150 °C. Superscript b signifies that 10 mol % of **Mg-2b** was used as the catalyst.

undergoes heterolytic cleavage by the magnesium center and the de-aromatized phosphine side arm. This step has an activation free energy of 23.0 kcal/mol, and it is endergonic by 2.4 kcal/mol, suggesting the high reactivity of the unobserved intermediate **B**. It should be mentioned that the activation of H_2 by intermediate **A′** derived from the dissociation of one dioxane from **Mg-2b** is also favorable according to the DFT studies (see page S85 in the SI). The active intermediate **B** is partially transformed into the dimeric complex **Mg-3**, as mentioned above in the control experiments (Figure 3e). Insertion of imine **1a** into the Mg−H bond of intermediate **B** produces intermediate **Mg-4**, which is relatively stable and experimentally observed in the N−H bond activation reaction of **Mg-2a** with amine **2a** (Figure 3f). It is noted that using the *in situ*-generated **Mg-4** as a catalyst for the hydrogenation of **1a**, 81% yield of **2a** was obtained under the standard conditions, suggesting that **Mg-4** is involved in the catalytic cycle. The monitoring experiments using **Mg-2a** as a catalyst further confirmed that **Mg-4** is a key intermediate in catalytic reaction (Figure S57). DFT studies also indicate that the formation of **Mg-4** is an exergonic step (ΔG = −28.3 kcal/mol) with a free energy barrier of 7.8 kcal/mol to overcome transition state **TS-II**. The next step is the proton migration from the phosphine side arm of intermediate **Mg-4** to the bound amine to give the de-aromatized intermediate **C** with the secondary amine coordinating to the magnesium center. This step is an endergonic process with ΔG = 7.1 kcal/mol and a transition state **TS-III** with a free energy barrier of 18.5 kcal/mol. Finally, the amine product **2a** is released from intermediate **C** to regenerate the four-coordinated intermediate **A** to propagate the cycle, which is endergonic (ΔG = 5.4 kcal/mol). The DFT studies highlight the significance of MLC in this reaction.

Catalytic Hydrogenation of *N*-Heteroarenes. The successful hydrogenation of imines catalyzed by the de-aromatized magnesium complexes encouraged us to extend the developed catalysis to the hydrogenation of other compounds that contain C═N bond. Selective hydrogenation of quinolines and their closely related *N*-heteroarenes is an efficient way to access tetrahydroquinolines and related compounds, which are ubiquitous in natural products and drugs. Homogeneously catalyzed hydrogenation under mild conditions based on precious metals has been developed.[26] In recent years, FLPs[5d] and first-row transition metals[15] have been reported to catalyze the hydrogenation of *N*-heteroarenes, avoiding the use of noble metals. However, to the best of our knowledge, the utilization of early main-group metal catalysts in this field has never been documented. The de-aromatized magnesium complexes may be capable of catalyzing the hydrogenation of quinolines and related *N*-heteroarenes. Surprisingly, under the same conditions as the imine hydrogenation, quinoline **3a** was smoothly converted into tetrahydroquinoline **4a** in 92% isolated yield catalyzed by **Mg-2b** (Figure 6). Substituted quinolines with a series of functional groups at different positions successfully afforded the desired cyclic amines (**4b**−**4w**). It is worth mentioning that

https://doi.org/10.1021/jacs.3c01091
J. Am. Chem. Soc. 2023, 145, 9164−9175

the racemic noralkaloids **4c** was obtained in 87% yield, which can be converted to (±)-angustureine followed by methylation.[27] Reducible functional groups, such as alkene and alkyne, were not affected in the current catalysis (**4t** and **4u**), showing great significance in organic synthesis. It is noted that 8-substituted quinoline (**3w**) generated relatively lower yields than others, probably because of its more steric hindrance. Other *N*-heteroarenes, including isoquinolines (**3x** and **3y**), quinoxalines (**3z**−**3ab**), and 7,8-benzoquinoline (**3ac**), were hydrogenated at 150 °C, generating corresponding products in high yields. These results indicated that the de-aromatized complexes are not only suitable for the hydrogenation of imines but also efficient in the selective hydrogenation of *N*-heteroarenes.

CONCLUSIONS

In summary, we have developed a series of new de-aromatized magnesium pincer complexes by using the PNNH-type ligands. The complexes were well-characterized and are relatively stable compared to the reported Mg(PNP) complexes. Activation of H−H and N−H bonds by the de-aromatized complexes via an MLC process was demonstrated. The new magnesium pincer complexes were applied to the catalytic hydrogenation of various aldimines to generate secondary amines in excellent yields, providing a new strategy for the hydrogenation of imines using magnesium complexes. It is noted that, compared to previously reported hydrogenation of aldimines catalyzed by magnesium complexes, the reaction reported here represents a broader scope and higher yields. In addition, the developed complexes are efficient in the hydrogenation of ketimines, offering a successful example of homogeneous early main-group metal-catalyzed hydrogenation of ketimines. Mechanistic studies indicate that the aromatization/de-aromatization MLC process plays a significant role in achieving imine hydrogenation, as supported by control experiments and DFT studies. Furthermore, the developed catalysis is extended to the selective hydrogenation of *N*-heteroarenes, showing an unprecedented example of early main-group metal homogeneously catalyzed hydrogenation of *N*-heteroarenes. A variety of functional groups, including the fluoro, chloro, and C−C double and triple bonds, are well tolerated in the developed system. This study is a significant advancement in main-group metal catalysis and C═N bond hydrogenation. We believe that it will inspire the area of main-group metal chemistry and hydrogenation reactions.

ASSOCIATED CONTENT

Supporting Information

The Supporting Information is available free of charge at https://pubs.acs.org/doi/10.1021/jacs.3c01091.

Experimental procedures, NMR spectra, and computational details (PDF)

Accession Codes

CCDC 2237494−2237497 contain the supplementary crystallographic data for this paper. These data can be obtained free of charge via www.ccdc.cam.ac.uk/data_request/cif, or by emailing data_request@ccdc.cam.ac.uk, or by contacting The Cambridge Crystallographic Data Centre, 12 Union Road, Cambridge CB2 1EZ, UK; fax: +44 1223 336033.

AUTHOR INFORMATION

Corresponding Author

David Milstein − *Department of Molecular Chemistry and Materials Science, Weizmann Institute of Science, Rehovot 7610001, Israel;* orcid.org/0000-0002-2320-0262; Email: david.milstein@weizmann.ac.il

Authors

Yaoyu Liang − *Department of Molecular Chemistry and Materials Science, Weizmann Institute of Science, Rehovot 7610001, Israel*

Jie Luo − *Department of Molecular Chemistry and Materials Science, Weizmann Institute of Science, Rehovot 7610001, Israel*

Yael Diskin-Posner − *Department of Chemical Research Support, Weizmann Institute of Science, Rehovot 7610001, Israel;* orcid.org/0000-0002-9008-8477

Complete contact information is available at: https://pubs.acs.org/10.1021/jacs.3c01091

Notes

The authors declare no competing financial interest.

ACKNOWLEDGMENTS

J. L. is thankful to the Feinberg Graduate School of Weizmann Institute of Science for a Senior Postdoctoral Fellowship.

REFERENCES

(1) (a) Jäkel, C.; Paciello, R. High-Throughput and Parallel Screening Methods in Asymmetric Hydrogenation. *Chem. Rev.* **2006**, *106*, 2912−2942. ((b)) de Vries, J. G.; Elsevier, C. J. *The Handbook of Homogeneous Hydrogenation;* Wiley-VCH, Weinheim, 2007; pp. 2−256. ((c)) Claver, C.; Fernández, E. *Modern Reduction Methods*; Wiley-VCH, Winheim, 2008.

(2) (a) Xie, J.-H.; Zhu, S.-F.; Zhou, Q.-L. Transition Metal-Catalyzed Enantioselective Hydrogenation of Enamines and Imines. *Chem. Rev.* **2011**, *111*, 1713−1760. (b) Zhao, B.; Han, Z.; Ding, K. The N−H Functional Group in Organometallic Catalysis. *Angew. Chem., Int. Ed.* **2013**, *52*, 4744−4788. (c) Chen, Q.-A.; Ye, Z.-S.; Duan, Y.; Zhou, Y.-G. Homogeneous Palladium-Catalyzed Asymmetric Hydrogenation. *Chem. Soc. Rev.* **2013**, *42*, 497−511. (d) Gunanathan, C.; Milstein, D. Bond Activation and Catalysis by Ruthenium Pincer Complexes. *Chem. Rev.* **2014**, *114*, 12024−12087.

(3) For selected reviews of using first-row transition metals in catalytic hydrogenations, see (a) Zell, T.; Milstein, D. Hydrogenation and Dehydrogenation Iron Pincer Catalysts Capable of Metal-Ligand Cooperation by Aromatization/Dearomatization. *Acc. Chem. Res.* **2015**, *48*, 1979−1994. (b) Chirik, P. J. Iron- and Cobalt-Catalyzed Alkene Hydrogenation: Catalysis with Both Redox-Active and Strong Field Ligands. *Acc. Chem. Res.* **2015**, *48*, 1687−1695. (c) Chakraborty, S.; Bhattacharya, P.; Dai, H.; Guan, H. Nickel and Iron Pincer Complexes as Catalysts for the Reduction of Carbonyl Compounds. *Acc. Chem. Res.* **2015**, *48*, 1995−2003. (d) Wei, D.; Darcel, C. Iron Catalysis in Reduction and Hydrometalation Reactions. *Chem. Rev.* **2019**, *119*, 2550−2610. (e) Wang, Y.; Wang, M.; Li, Y.; Liu, Q. Homogeneous Manganese-Catalyzed Hydrogenation and Dehydrogenation Reactions. *Chem* **2021**, *7*, 1180−1223.

(4) Zinc is considered as a main-group metal in some literatures. For zinc-catalyzed hydrogenation reactions, see (a) Werkmeister, S.; Fleischer, S.; Junge, K.; Beller, M. Towards a Zinc-Catalyzed Asymmetric Hydrogenation/Transfer Hydrogenation of Imines. *Chem. − Asian J.* **2012**, *11*, 2562−2568. (b) Werkmeister, S.; Fleischer, S.; Zhou, S.; Junge, K.; Beller, M. Development of New Hydrogenations of Imines and Benign Reductive Hydroaminations: Zinc Triflate as a Catalyst. *ChemSusChem* **2012**, *5*, 777−782. (c) Jochmann, P.; Stephan, D. W. H_2 Cleavage, Hydride Formation,

and Catalytic Hydrogenation of Imines with Zinc Complexes of C_5Me_5 and *N*-Heterocyclic Carbenes. *Angew. Chem., Int. Ed.* **2013**, *52*, 9831−9835. (d) Jochmann, P.; Stephan, D. W. Zincocene and Dizincocene *N*-Heterocyclic Carbene Complexes and Catalytic Hydrogenation of Imines and Ketones. *Chem. − Eur. J.* **2014**, *20*, 8370−8378. (e) Rauch, M.; Kar, S.; Kumar, A.; Avram, L.; Shimon, L. J. W.; Milstein, D. Metal-Ligand Cooperation Facilitates Bond Activation and Catalytic Hydrogenation with Zinc Pincer Complexes. *J. Am. Chem. Soc.* **2020**, *142*, 14513−14521.

(5) For selected reviews of using FLPs in catalytic hydrogenations, see (a) Stephan, D. W. Frustrated Lewis Pairs: From Concept to Catalysis. *Acc. Chem. Res.* **2015**, *48*, 306−316. (b) Stephan, D. W.; Erker, G. Frustrated Lewis Pair Chemistry: Development and Perspectives. *Angew. Chem., Int. Ed.* **2015**, *54*, 6400−6441. (c) Stephan, D. W. Boron-Based Frustrated Lewis Pairs in Hydrogenation Catalysis. *PATAI'S Chem.Funct. Groups* **2019**, 1. (d) Lam, J.; Szkop, K. M.; Mosaferi, E.; Stephan, D. W. FLP Catalysis: Main Group Hydrogenations of Organic Unsaturated Substrates. *Chem. Soc. Rev.* **2019**, *48*, 3592−3612. For selected examples, see: (e) Chase, P. A.; Welch, G. C.; Jurca, T.; Stephan, D. W. Metal-Free Catalytic Hydrogenation. *Angew. Chem., Int. Ed.* **2007**, *46*, 8050−8053. (f) Hatnean, J. A.; Thomson, J. W.; Chase, P. A.; Stephan, D. W. Imine Hydrogenation by Alkylaluminum Catalysts. *Chem. Commun.* **2014**, *50*, 301−303. (g) Xu, M.; Jupp, A. R.; Qu, Z.-W.; Stephan, D. W. Alkali Metal Species in the Reversible Activation of H_2. *Angew. Chem., Int. Ed.* **2018**, *57*, 11050−11054.

(6) (a) Harder, S. *Early Main Group Metal Catalysis: Concepts and Reactions*; Wiley-VCH Verlag, 2020; pp. 175−199. (b) Harder, S. Molecular Early Main Group Metal Hydrides: Synthetic Challenge Structures and Applications. *Chem. Commun.* **2012**, *48*, 11165−11177. (c) Revunova, K.; Nikonov, G. I. Main Group Catalyzed Reduction of Unsaturated Bonds. *Dalton Trans.* **2015**, *44*, 840−866. (d) Magre, M.; Szewczyk, M.; Rueping, M. Magnesium Complexes in Hydroelementation and Reduction Catalysis: Opportunities and Challenges. *Curr. Opin. Green Sustainable Chem.* **2021**, *32*, 100526. (e) Roy, M. M. D.; Omaña, A. A.; Wilson, A. S. S.; Hill, M. S.; Aldridge, S.; Rivard, E. Molecular Main Group Metal Hydrides. *Chem. Rev.* **2021**, *121*, 12784−12965. (f) Orr, S. A.; Andrews, P. C.; Blair, V. L. Main Group Metal-Mediated Transformations of Imines. *Chem. − Eur. J.* **2021**, *27*, 2569−2588.

(7) (a) Walling, C.; Bollyky, L. Base Catalyzed Homogeneous Hydrogenation. *J. Am. Chem. Soc.* **1961**, *83*, 2968−2969. (b) Walling, C.; Bollyky, L. Homogeneous Hydrogenation in the Absence of Transition-Metal Catalysts. *J. Am. Chem. Soc.* **1964**, *86*, 3750−3752. (c) Slaugh, L. H. Metal Hydrides. Hydrogenation and Isomerization Catalysis. *J. Org. Chem.* **1967**, *32*, 108−113.

(8) (a) Spielman, J.; Buch, F.; Harder, S. Early Main-Group Metal Catalysts for the Hydrogenation of Alkenes with H_2. *Angew. Chem., Int. Ed.* **2008**, *47*, 9434−9438. (b) Jochmann, P.; Davin, J. P.; Spaniol, T. P.; Maron, L.; Okuda, J. A Cationic Calcium Hydride Cluster Stabilized by Cyclen-Derived Macrocyclic N,N,N, N Ligands. *Angew. Chem., Int. Ed.* **2012**, *51*, 4452−4455. (c) Schuhknecht, D.; Lhotžky, C.; Spaniol, T. P.; Maron, L.; Okuda, J. Calcium Hydride Cation $[CaH]^+$ Stabilized by an NNNN-Type Macrocyclic Ligand: A Selective Catalyst for Olefin Hydrogenation. *Angew. Chem., Int. Ed.* **2017**, *56*, 12367−12371. (d) Wilson, A. S. S.; Dinoi, C.; Hill, M. S.; Mahon, M. F.; Maron, L. Heterolysis of Dihydrogen by Nucleophilic Calcium Alkyls. *Angew. Chem., Int. Ed.* **2018**, *57*, 15500−15504. (e) Shi, X.; Qin, Y.; Wang, Y.; Zhao, L.; Liu, Z.; Cheng, J. Super-Bulky Penta-Arylcyclopentadienyl Ligands: Isolation of the Full Range of Half-Sandwich Heavy Alkaline-Earth Metal Hydrides. *Angew. Chem., Int. Ed.* **2019**, *58*, 4356−4360. (f) Shi, X.; Cheng, J. Reversible Addition and Hydrogenation of 1,1-Diphenylethylene with A Barium Complex. *Dalton Trans.* **2019**, *48*, 8565−8568. (g) Shi, X.; Hou, C.; Zhao, L.; Deng, P.; Cheng, J. Mononuclear Calcium Complex as Effective Catalyst for Alkenes Hydrogenation. *Chem. Commun.* **2020**, *56*, 5162−5165. (h) Höllerhage, T.; Schuhknecht, D.; Mistry, A.; Spaniol, T. P.; Yang, Y.; Maron, L.; Okuda, J. Calcium Hydride Catalysts for Olefin Hydrofunctionalization: Ring-Size Effect of Macrocyclic Ligands on Activity. *Chem. − Eur. J.* **2021**, *27*, 3002−3007.

(9) (a) Bauer, H.; Alonso, M.; Fischer, C.; Rösch, B.; Elsen, H.; Harder, S. Simple Alkaline-Earth Metal Catalysts for Effective Alkene Hydrogenation. *Angew. Chem., Int. Ed.* **2018**, *57*, 15177−15182. (b) Bauer, H.; Alonso, M.; Färber, C.; Elsen, H.; Pahl, J.; Causero, A.; Ballmann, G.; Proft, F. D.; Harder, S. Imine Hydrogenation with Simple Alkaline Earth Metal Catalysts. *Nat. Catal.* **2018**, *1*, 40−47. (c) Elliott, D. C.; Marti, A.; Mauleón, P.; Pfaltz, A. H_2 Activation by Non-Transition-Metal Systems: Hydrogenation of Aldimines and Ketimines with $LiN(SiMe_3)_2$. *Chem. − Eur. J.* **2019**, *25*, 1918−1922. (d) Martin, J.; Knüpfer, C.; Eyselein, J.; Färber, C.; Grams, S.; Langer, J.; Thum, K.; Wiesinger, M.; Harder, S. Highly Active Superbulky Alkaline Earth Metal Amide Catalysts for Hydrogenation of Challenging Alkenes and Aromatic Rings. *Angew. Chem., Int. Ed.* **2020**, *59*, 9102−9112.

(10) Friedrich, A.; Eyselein, J.; Elsen, H.; Langer, J.; Pahl, J.; Wiesinger, M.; Harder, S. Cationic Aluminium Complexes as Catalysts for Imine Hydrogenation. *Chem. − Eur. J.* **2021**, *27*, 7756−7763.

(11) (a) Elsen, H.; Färber, C.; Ballmann, G.; Harder, S. $LiAlH_4$: From Stoichiometric Reduction to Imine Hydrogenation Catalysis. *Angew. Chem., Int. Ed.* **2018**, *57*, 7156−7160. (b) Zhang, X.-Y.; Du, H.-Z.; Zhai, D.-D.; Guan, B.-T. Combined KH/Alkaline-Earth Metal Amide Catalysts for Hydrogenation of Alkenes. *Org. Chem. Front.* **2020**, *7*, 1991−1996. (c) Elsen, H.; Langer, J.; Wiesinger, M.; Harder, S. Alkaline Earth Metal Aluminates as Catalysts for Imine Hydrogenation. *Organometallics* **2020**, *39*, 4238−4246. (d) Wiesinger, M.; Knüpfer, C.; Elsen, H.; Mai, J.; Langer, J.; Harder, S. Heterometallic Mg-Ba Hydride Clusters in Hydrogenation Catalysis. *ChemCatChem* **2021**, *13*, 4567−4577.

(12) Liang, Y.; Das, U. K.; Luo, J.; Posner-Diskin, Y.; Avram, L.; Milstein, D. Magnesium Pincer Complexes and Their Applications in Catalytic Semihydrogenation of Alkynes and Hydrogenation of Alkenes: Evidence for Metal−Ligand Cooperation. *J. Am. Chem. Soc.* **2022**, *144*, 19115−19126.

(13) (a) Wang, C.; Villa-Marcos, B.; Xiao, J. Hydrogenation of Imino Bonds with Half-Sandwich Metal Catalysts. *Chem. Commun.* **2011**, *47*, 9773−9785. (b) Fabrello, A.; Bachelier, A.; Urrutigoïty, M.; Kalck, P. Mechanistic Analysis of the Transition Metal-Catalyzed Hydrogenation of Imines and Functionalized Enamines. *Coord. Chem. Rev.* **2010**, *254*, 273−287. (c) Sridharan, V.; Suryavanshi, P. A.; Menéndez, J. C. Advances in the Chemistry of Tetrahydroquinolines. *Chem. Rev.* **2011**, *111*, 7157−7259. (d) Muthukrishnan, I.; Sridharan, V.; Menéndez, J. C. Progress in the Chemistry of Tetrahydroquinolines. *Chem. Rev.* **2019**, *119*, 5057−5191. (e) El-Shahat, M. Advances in the Reduction of Quinolines to 1,2,3,4-Tetrahydroquinolines. *J. Heterocyclic Chem.* **2022**, *59*, 399−421.

(14) For selected examples of using the first-row transition metals in imines hydrogenation, see (a) Zhang, G.; Scott, B. L.; Hanson, S. K. Mild and Homogeneous Cobalt-Catalyzed Hydrogenation of C=C, C=O, and C=N Bonds. *Angew. Chem., Int. Ed.* **2012**, *51*, 12102−12106. (b) Gärtner, D.; Welther, A.; Rad, B. R.; Wolf, R.; von Wangelin, A. J. Heteroatom-Free Arene-Cobalt and Arene-Iron Catalysts for Hydrogenations. *Angew. Chem., Int. Ed.* **2014**, *53*, 3722−3726. (c) Freitag, F.; Irrgang, T.; Kempe, R. Mechanistic Studies of Hydride Transfer to Imines from a Highly Active and Chemoselective Manganate Catalyst. *J. Am. Chem. Soc.* **2019**, *141*, 11677−11685. (d) Li, B.; Chen, J.; Zhang, Z.; Gridnev, I. D.; Zhang, W. Nickel-Catalyzed Asymmetric Hydrogenation of *N*-Sulfonyl Imines. *Angew. Chem., Int. Ed.* **2019**, *58*, 7329−7334. (e) Wang, Y.; Liu, S.; Yang, H.; Li, H.; Lan, Y.; Liu, Q. Structure, Reactivity and Catalytic Properties of Manganese-Hydride Amidate Complexes. *Nat. Chem.* **2022**, *14*, 1233−1241.

(15) For first-row transition metals catalyzed hydrogenation of *N*-heteroarenes, see (a) Chakraborty, S.; Brennessel, W. W.; Jones, W. D. A Molecular Iron Catalyst for the Acceptorless Dehydrogenation and Hydrogenation of *N*-Heterocycles. *J. Am. Chem. Soc.* **2014**, *136*, 8564−8567. (b) Xu, R.; Chakraborty, S.; Yuan, H.; Jones, W. D.

https://doi.org/10.1021/jacs.3c01091
J. Am. Chem. Soc. 2023, 145, 9164−9175

Acceptorless, Reversible Dehydrogenation and Hydrogenation of *N*-Heterocycles with a Cobalt Pincer Catalyst. *ACS Catal.* **2015**, *5*, 6350−6354. (c) Adam, R.; Cabrero-Antonino, J. R.; Spannenberg, A.; Junge, K.; Jackstell, R.; Beller, M. A General and Highly Selective Cobalt-Catalyzed Hydrogenation of *N*-Heteroarenes under Mild Reaction Conditions. *Angew. Chem., Int. Ed.* **2017**, *56*, 3216−3220. (d) Sandl, S.; Maier, T. M.; van Leest, N. P.; Kröncke, S.; Chakraborty, U.; Demeshko, S.; Koszinowski, K.; de Bruin, B.; Meyer, F.; Bodensteiner, M.; Herrmann, C.; Wolf, R.; Jacobi von Wangelin, A. Cobalt-Catalyzed Hydrogenations via Olefin Cobaltate and Hydride Intermediates. *ACS Catal.* **2019**, *9*, 7596−7606. (e) Wang, Y.; Zhu, L.; Shao, Z.; Li, G.; Lan, Y.; Liu, Q. Unmasking the Ligand Effect in Manganese-Catalyzed Hydrogenation: Mechanistic Insight and Catalytic Application. *J. Am. Chem. Soc.* **2019**, *141*, 17337−17349. (f) Duan, Y.-N.; Du, X.; Cui, Z.; Zeng, Y.; Liu, Y.; Yang, T.; Wen, J.; Zhang, X. Homogeneous Hydrogenation with a Cobalt/Tetraphosphine Catalyst: A Superior Hydride Donor for Polar Double Bonds and *N*-Heteroarenes. *J. Am. Chem. Soc.* **2019**, *141*, 20424−20433. (g) Papa, V.; Cao, Y.; Spannenberg, A.; Junge, K.; Beller, M. Development of a Practical Non-Noble Metal Catalyst for Hydrogenation of *N*-Heteroarenes. *Nat. Catal.* **2020**, *3*, 135−142.

(16) (a) Magre, M.; Szewczyk, M.; Rueping, M. s-Block Metal Catalysts for the Hydroboration of Unsaturated Bonds. *Chem. Rev.* **2022**, *122*, 8261−8312. (b) Hill, M. S.; Liptrot, D. J.; Weetman, C. Alkaline Earths as Main Group Reagents in Molecular Catalysis. *Chem. Soc. Rev.* **2016**, *45*, 972−988. (c) Rochat, R.; Lopez, M. J.; Tsurugi, H.; Mashima, K. Recent Developments in Homogeneous Organomagnesium Catalysis. *ChemCatChem* **2016**, *8*, 10−20.

(17) For magnesium catalyzed hydroamination, see (a) Crimmin, M. R.; Arrowsmith, M.; Barrett, A. G. M.; Casely, I. J.; Hill, M. S.; Procopiou, P. A. Intramolecular Hydroamination of Aminoalkenes by Calcium and Magnesium Complexes: A Synthetic and Mechanistic Study. *J. Am. Chem. Soc.* **2009**, *131*, 9670−9685. (b) Dunne, J. F.; Fulton, D. B.; Ellern, A.; Sadow, A. D. Concerted C−N and C−H Bond Formation in a Magnesium-Catalyzed Hydroamination. *J. Am. Chem. Soc.* **2010**, *132*, 17680−17683. (c) Zhang, X.; Emge, T. J.; Hultzsch, K. C. Intramolecular Aminoalkene Hydroamination Catalyzed by Magnesium Complexes Containing Multidentate Phenoxyamine Ligands. *Organometallics* **2010**, *29*, 5871−5877. (d) Zhang, X.; Emge, T. J.; Hultzsch, K. C. A Chiral Phenoxyamine Magnesium Catalyst for the Enantioselective Hydroamination/Cyclization of Aminoalkenes and Intermolecular Hydroamination of Vinyl Arenes. *Angew. Chem., Int. Ed.* **2012**, *51*, 394−398. (e) Arrowsmith, M.; Hill, M. S.; Kociok-Köhn, G. Dearomatized BIAN Alkaline-Earth Alkyl Catalysts for the Intramolecular Hydroamination of Hindered Aminoalkenes. *Organometallics* **2014**, *33*, 206−216.

(18) For magnesium catalyzed hydrosilylation, see (a) Lampland, N. L.; Pindwal, A.; Neal, S. R.; Schlauderaff, S.; Ellern, A.; Sadow, A. D. Magnesium-Catalyzed Hydrosilylation of α,β-Unsaturated Esters. *Chem. Sci.* **2015**, *6*, 6901−6907. (b) Anker, M. D.; Hill, M. S.; Lowe, J. P.; Mahon, M. F. Alkaline-Earth-Promoted CO Homologation and Reductive Catalysis. *Angew. Chem., Int. Ed.* **2015**, *54*, 10009−10011. (c) Rauch, M.; Ruccolo, S.; Parkin, G. Synthesis, Structure, and Reactivity of a Terminal Magnesium Hydride Compound with a Carbatrane Motif, [Tism^{PriBenz}]MgH: A Multifunctional Catalyst for Hydrosilylation and Hydroboration. *J. Am. Chem. Soc.* **2017**, *139*, 13264−13267. (d) Gercia, L.; Dinoi, C.; Mahon, M. F.; Maron, L.; Hill, M. S. Magnesium Hydride Alkene Insertion and Catalytic Hydrosilylation. *Chem. Sci.* **2019**, *10*, 8108−8118. (e) Garcia, L.; Mahon, M. F.; Hill, M. S. Multimetallic Alkaline-Earth Hydride Cations. *Organometallics* **2019**, *38*, 3778−3785.

(19) For selected examples of magnesium catalyzed hydroboration, see (a) Arrowsmith, M.; Hill, M. S.; Hadlington, T.; Kociok-köhn, G.; Weetman, C. Magnesium-Catalyzed Hydroboration of Pyridines. *Organometallics* **2011**, *30*, 5556−5559. (b) Mukherjee, D.; Ellern, A.; Sadow, A. D. Magnesium-Catalyzed Hydroboration of Esters: Evidence for a New Zwitterionic Mechanism. *Chem. Sci.* **2014**, *5*, 959−964. (c) Fohlmeister, L.; Stasch, A. Ring-Shaped PhosphinoamidoMagnesium-Hydride Complexes: Syntheses, Structures, Reactivity, and Catalysis. *Chem. − Eur. J.* **2016**, *22*, 10235−10246. (d) Magre, M.; Maity, B.; Falconnet, A.; Cavallo, L.; Rueping, M. Magnesium-Catalyzed Hydroboration of Terminal and Internal Alkynes. *Angew. Chem., Int. Ed.* **2019**, *58*, 7025−7029. (e) Magre, M.; Paffenholz, E.; Maity, B.; Cavallo, L.; Rueping, M. Regiodivergent Hydroborative Ring Opening of Epoxides via Selective C−O Bond Activation. *J. Am. Chem. Soc.* **2020**, *142*, 14286−14294.

(20) For magnesium catalyzed dehydrocoupling reactions, see (a) Spielmann, J.; Bolte, M.; Harder, S. Synthesis and Structure of A Magnesium−Amidoborane Complex and Its Role in Catalytic Formation of A New Bis-Aminoborane Ligand. *Chem. Commun.* **2009**, 6934−6936. (b) Dunne, J. F.; Neal, S. R.; Engelkemier, J.; Ellern, A.; Sadow, A. D. Tris(oxazolinyl)boratomagnesium-Catalyzed Cross-Dehydrocoupling of Organosilanes with Amines, Hydrazine, and Ammonia. *J. Am. Chem. Soc.* **2011**, *133*, 16782−16785. (c) Liptrot, D. J.; Hill, M. S.; Mahon, M. F. Accessing the Single-Electron Manifold: Magnesium-Mediated Hydrogen Release from Silanes. *Angew. Chem., Int. Ed.* **2014**, *53*, 6224−6227. (d) Liptrot, D. J.; Hill, M. S.; Mahon, M. F.; Wilson, A. S. S. Alkaline-Earth-Catalyzed Dehydrocoupling of Amines and Boranes. *Angew. Chem., Int. Ed.* **2015**, *54*, 13362−13365.

(21) (a) Gunanathan, C.; Milstein, D. Metal−Ligand Cooperation by Aromatization-Dearomatization: A New Paradigm in Bond Activation and "Green" Catalysis. *Acc. Chem. Res.* **2011**, *44*, 588−602. (b) Khusnutdinova, J. R.; Milstein, D. Metal−Ligand Cooperation. *Angew. Chem., Int. Ed.* **2015**, *54*, 12236−12273. (c) Mukherjee, A.; Milstein, D. Homogeneous Catalysis by Cobalt and Manganese Pincer Ccomplexes. *ACS Catal.* **2018**, *8*, 11435−11469. (d) Alig, L.; Fritz, M.; Schneider, S. First-Row Transition Metal (De)Hydrogenation Catalysis Based on Functional Pincer Ligands. *Chem. Rev.* **2019**, *119*, 2681−2751.

(22) In previously reported magnesium complexes, the $^{31}P\{^{1}H\}$ NMR chemical shifts of the deprotonated phosphine side arm (close to 0 ppm) appear at higher fields than the protonated side arm (close to 20 ppm).

(23) (a) Green, S. P.; Jones, C.; Stasch, A. Stable Adducts of a Dimeric Magnesium(I) Compound. *Angew. Chem., Int. Ed.* **2008**, *47*, 9079−9083. (b) Martin, D.; Beckerle, K.; Schnitžler, S.; Spaniol, T. P.; Maron, L.; Okuda, J. Discrete Magnesium Hydride Aggregates: A Cationic $Mg_{13}H_{18}$ Cluster Stabilized by NNNN-Type Macrocycles. *Angew. Chem., Int. Ed.* **2015**, *54*, 4115−4118.

(24) (a) Fogle, E.; Garg, J. A.; Hu, P.; Leitus, G.; Shimon, L. J. W.; Milstein, D. System with Potential Dual Modes of Metal−Ligand Cooperation: Highly Catalytically Active Pyridine-Based PNNH−Ru Pincer Complexes. *Chem. − Eur. J.* **2014**, *20*, 15727−15731. (b) Espinosa-Jalapa, N. A.; Kumar, A.; Leitus, G.; Posner-Diskin, Y.; Milstein, D. Synthesis of Cyclic Imides by Acceptorless Dehydrogenative Coupling of Diols and Amines Catalyzed by a Manganese Pincer Complex. *J. Am. Chem. Soc.* **2017**, *139*, 11722−11725. (c) Srimani, D.; Mukherjee, A.; Goldberg, A. F. G.; Leitus, G.; Diskin-Posner, Y.; Shimon, L. J. W.; Ben-David, Y.; Milstein, D. Cobalt-Catalyzed Hydrogenation of Esters to Alcohols: Unexpected Reactivity Trend Indicates Ester Enolate Intermediacy. *Angew. Chem., Int. Ed.* **2015**, *54*, 12357−12360.

(25) N−H bond activation by main-group compounds has been reported; For selected examples, see (a) Dankert, F.; Siewert, J.-E.; Cupta, P.; Weigend, F.; Junghans-Hering, C. Metal-Free N−H Bond Activation by Phospha-Wittig Reagents. *Angew. Chem., Int. Ed.* **2022**, *61*, No. e202207064. (b) Cui, J.; Li, Y.; Canguly, R.; Inthirarajah, A.; Hirao, H.; Kinjo, R. Metal-Free σ-Bond Metathesis in Ammonia Activation by a Diazadiphosphapentalene. *J. Am. Chem. Soc.* **2014**, *136*, 16764−16767.

(26) For selected examples, see (a) Wang, W.-B.; Lu, S.-M.; Yang, P.-Y.; Han, X.-W.; Zhou, Y.-G. Highly Enantioselective Iridium-Catalyzed Hydrogenation of Heteroaromatic Compounds, Quinolines. *J. Am. Chem. Soc.* **2003**, *125*, 10536−10537. (b) Qiu, L.; Kwong, F. Y.; Wu, J.; Lam, W. H.; Chan, S.; Yu, W. Y.; Li, Y. M.; Guo, R.; Zhou, Z.; Chan, A. S. C. A New Class of Versatile Chiral-Bridged Atropisomeric Diphosphine Ligands: Remarkably Efficient Ligand Syntheses and Their Applications in Highly Enantioselective Hydro-

https://doi.org/10.1021/jacs.3c01091
J. Am. Chem. Soc. 2023, 145, 9164−9175

genation Reactions. *J. Am. Chem. Soc.* **2006**, *128*, 5955−5965. (c) Dobereiner, G. E.; Nova, A.; Schley, N. D.; Hazari, N.; Miller, S. J.; Eisenstein, O.; Crabtree, R. H. Iridium-Catalyzed Hydrogenation of *N*-Heterocyclic Compounds under Mild Conditions by an Outer-Sphere Pathway. *J. Am. Chem. Soc.* **2011**, *133*, 7547−7562. (d) Ma, W.; Zhang, J.; Xu, C.; Chen, F.; He, Y.-M.; Fan, Q.-H. Highly Enantioselective Direct Synthesis of Endocyclic Vicinal Diamines through Chiral Ru(diamine)-Catalyzed Hydrogenation of 2,2'-Bisquinoline Derivatives. *Angew. Chem., Int. Ed.* **2016**, *55*, 12891−12894.

(27) Shahane, S.; Louafi, F.; Moreau, J.; Hurvois, J.-P.; Renaud, J.-L.; van de Weghe, P.; Roisnel, T. Synthesis of Alkaloids of Galipea *officinalis* by Alkylation of an α-Amino Nitrile. *Eur. J. Org. Chem.* **2008**, 4622−4631.

https://doi.org/10.1021/jacs.3c01091
J. Am. Chem. Soc. 2023, 145, 9164−9175